

Performance Analysis of a Dynamic Channel Switching Scheme in IMT-2000

Guidance

Professor	Masao FUKUSHIMA
Associate Professor	Tetsuya TAKINE

Shiro TSUCHIYAMA

2000 Graduate Course

in

Department of Applied Mathematics and Physics
Graduate School of Informatics, Kyoto University



February 2002

Abstract

The number of users of mobile communications systems has increased dramatically. In particular, mobile phones have thoroughly penetrated people's daily lives. And then, various services including video, voice, fax and data transmission are demanded. To meet these demands, the implementation of an advanced mobile communications system is required. International Telecommunication Union (ITU) is now formulating standards for International Mobile Telecommunication 2000 (IMT-2000) that is the next generation mobile communication system. It makes the following services possible: high transmission speed, high transmission quality and the realization of global services accessible anywhere in the world.

The dynamic channel switching scheme in Radio Network Controller (RNC) is proposed for IMT 2000. It has two types of channels, i.e., dedicated channels and a common channel, for data transmission. The dedicated channel is allocated to one User Equipment (UE) exclusively and provides high-quality data transmission without either delay or data loss. On the other hand, the common channel is shared by many UEs. These channels are dynamically allocated to UEs based on the control parameters set in Radio Resources Controller (RRC). The dynamic channel allocation realizes economical and efficient use of these channels.

In this thesis, we propose an approximate model of the dynamic channel switching system. We describe the model by a continuous-time finite-state Markov chain, and then we apply the efficient procedure called Replacement Process Approach to solve the stationary equations of the Markov chain. Through numerical experiments, we examine quantitative performance of the system, i.e., the frame dropping probability, the load of a dedicated channel and the frequency of channel reallocation. Using those results, we can choose the control parameters to realize the demanded performance of the system.

Contents

1	Introduction	1
2	Wideband CDMA	2
2.1	UMTS architecture	2
2.2	Radio interface protocol architecture	2
2.2.1	Overall protocol structure	2
2.2.2	RLC/MAC layer	3
3	Dynamic channel switching scheme	5
4	Model description	6
4.1	Dynamic channel switching model	6
4.1.1	Model introduction	6
4.1.2	Assumptions on arrivals and services	7
4.2	Approximate model	8
4.2.1	Model description	8
4.2.2	Mathematical description	9
5	Analysis	10
5.1	State set	10
5.2	State transitions	10
5.3	Stationary equations	16
6	Numerical algorithm	19
7	Numerical results	24
7.1	Efficiency of the proposed numerical procedure	24
7.2	Accuracy of approximate model	25
7.3	Impact of upper threshold	27
8	Conclusion	29

1 Introduction

The number of users of mobile communications systems has increased dramatically. In particular, mobile phones have thoroughly penetrated people's daily lives. And then, various services including video, voice, fax and data transmission are demanded. To meet these demands, the implementation of an advanced mobile communications system is required.

International Telecommunication Union (ITU) is now formulating standards for International Mobile Telecommunication 2000 (IMT-2000) that is the next generation mobile communication system. It makes the following services possible: high transmission speed, high transmission quality and the realization of global services accessible anywhere in the world.

The dynamic channel switching scheme in Radio Network Controller (RNC) is proposed for IMT 2000. It has two types of channels for data transmission: some dedicated channels and a common channel. The dedicated channel is allocated to one User Equipment (UE) exclusively and provides high quality data transmission without either delay or data loss. On the other hand, the common channel is shared by some UEs. Furthermore, dynamic allocation of these channels is performed based on the queue length, and it helps use radio resources efficiently. Thus, proper allocation of channels should be done as in the following way.

The common channel should be shared by as many UEs as possible. It helps accommodate many UEs in the limited radio resources and keep many dedicated channels available. To keep dedicated channels unused enables us to allocate them on demand. Furthermore, it has an economical advantage, reducing the extra costs of using them. Thus, dedicated channels should be allocated in the limited case in which UEs require high-speed data transmission beyond the capacity of the common channel shared by many UEs. Of course, traffic volume being changed, they should be reallocated dynamically at an appropriate time.

These controls (allocation and reallocation) are performed based on a decision of Radio Resources Controller (RRC) in RNC. Note that the performance of these controls depends on the control parameters set by RRC. Therefore, we should determine these parameters in such a way that the most efficient and economical use of radio resources and higher quality of data transmission are provided. Thus, we present the performance analysis of the dynamic channel switching scheme to obtain the appropriate control parameters in this thesis.

The rest of this thesis is organized as follows. Section 2 summarizes the radio interface protocol architecture specified in IMT-2000. Section 3 describes the dynamic channel switching scheme mentioned above, and in Section 4, the mathematical model of the scheme is presented. Section 5 provides a numerical solution method to which iterative algorithm called Replacement Process Approach (RPA) is applied. Section 6 describes algorithm steps to execute the proposed method, and numerical results are presented in section 7. Finally, the thesis is concluded in Section 8.

2 Wideband CDMA

2.1 UMTS architecture

To provide end users with the necessary service quality for multimedia communications, flexible and high-bit-rate capabilities are required. Universal Mobile telecommunications System (UMTS) is a new radio access network based on 5 MHz W-CDMA, and optimized for efficient support of the next generation multimedia services.

Figure 1 shows the general system architecture of UMTS outlined in [2]. It includes UEs, Universal Telecommunication Radio Access Network (UTRAN) and a core network. The functional layering of the UMTS system into access and non-access stratum implies a functional division between UTRAN and the core network; UTRAN handles all radio-specific procedure, whereas the core network handles the service-specific procedures.

Furthermore, the general architecture includes two general interfaces: The Iu interface between UTRAN and the core network, and the radio interface (Uu) between UTRAN and the UE. In Section 2.2, we will focus on the radio interface in UMTS.

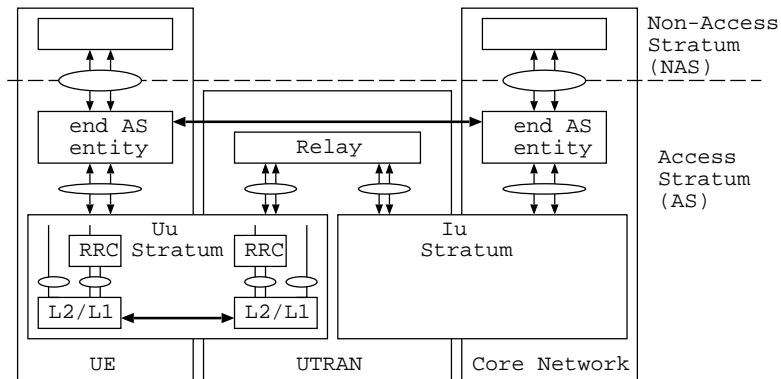


Figure 1: UMTS architecture.

2.2 Radio interface protocol architecture

2.2.1 Overall protocol structure

We first present the simple structure of the radio interface protocol specified in [3], which is layered into three protocol layers; the physical layer (Layer 1), the data link layer (Layer 2) and the network layer (Layer 3). Figure 2 shows its architecture.

The physical layer offers information transfer services to Medium Access Control (MAC). These services are provided at transport channels which are either common (i.e., shared among several users) or dedicated (i.e., allocated to a specific user). These two types of channels support multiple services fairly, for example, real-time services such as speech and packet data services. We will focus on the dynamic allocation of these channels in Section 3.

The data link layer is split into several sublayers. MAC and Radio Link Control (RLC) are described in the figure. MAC offers information transfer services to RLC. These services are provided at logical channels which are either control channel (i.e., transfer control information) or traffic channel (i.e., transfer user data). Furthermore, MAC performs the dynamic channel allocations mentioned above. These functions of MAC and RLC responsible for efficient data transmission are detailed in Section 2.2.2.

The network layer contains RRC which also plays a significant role in providing efficient data transmission. It offers control services to RLC, MAC and the physical layer. These services are provided at control Service Assess Points (SAPs) between RRC with the lower layers.

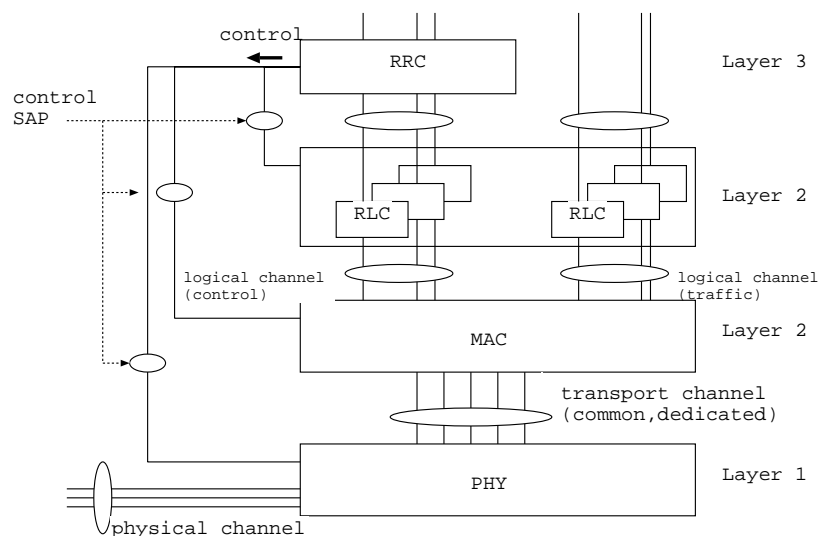


Figure 2: Radio interface protocol architecture.

2.2.2 RLC/MAC layer

We will focus on the RLC/MAC layers, which are responsible for efficient data transfer.

The RLC layer is responsible for establishment and release of layer 2 connections. The functions performed by the RLC include segmentation and assembly, error correction by retransmission, flow control, duplicate detection and in-sequence delivery of higher layer Protocol Data Units (PDUs)[5].

Figure 3 shows the segmentation and transformation of network layer packet data units. RLC Service Data Units (SDUs) are first segmented into RLC PDUs typically corresponding to the physical layer transport blocks. Each RLC PDU contains a sequence number used for low-level fast Automatic Repeat reQuest (ARQ). Therefore, RLC receiver checks sequence number when the PDUs are reassembled. If corrupted SDU is detected, retransmissions could be requested in acknowledged data transfer mode, or it will be simply discarded in unacknowledged data transfer mode. MAC mostly provides the following service: mapping between logical channels and transport channels, measurements of the system state, reporting the measurement results

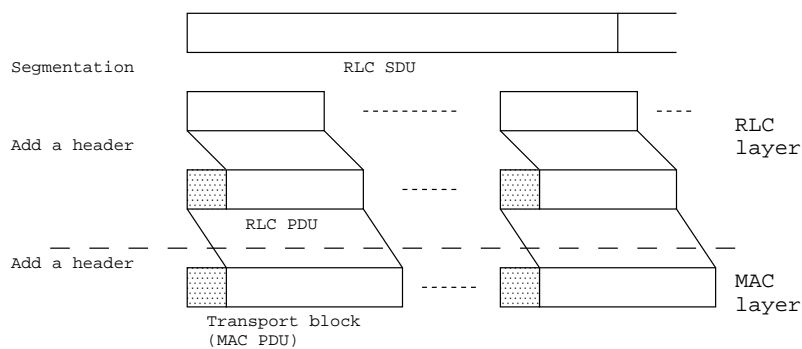


Figure 3: Segmentation and transformation of network layer packet data units.

to RRC, Reallocation of radio resources and flow control. We present these functions chiefly in view of the dynamic channel switching mechanism.

Logical channels are mapped into transport channels at MAC. Data delivered from RLC through logical channels is delivered to the physical layer through the transport channel. The transport channel is composed of the common transport channel and dedicated transport channels. The common transport channel is shared by some UEs, so that in-band identification of the UE is needed when particular UE is addressed. On the other hand, each dedicated channel is provided to one UE exclusively.

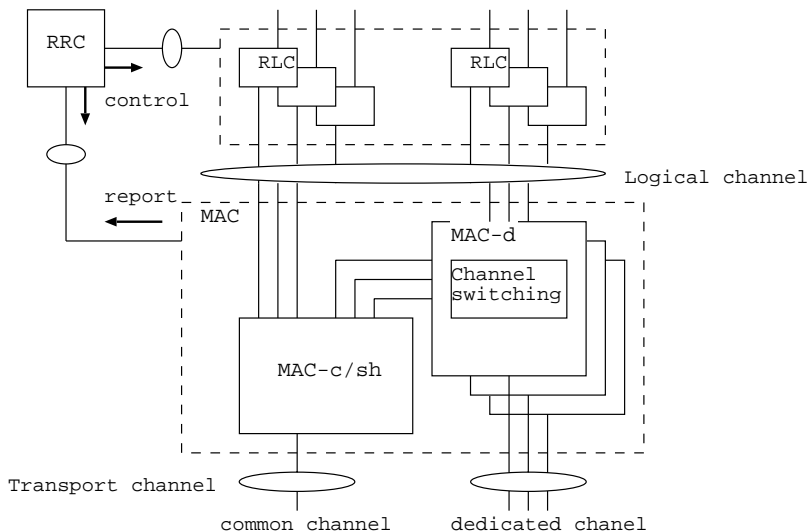


Figure 4: UTRAN side MAC architecture.

Figure 4 shows UTRAN side MAC architecture related with higher layers. MAC is constructed from one MAC-c/sh (Common MAC) entity and some MAC-d (Dedicated MAC) entities provided for each UE. MAC-c/sh controls access to the common transport channel. MAC-d controls access to dedicated transport channels. MAC-d can also switch transport channel type based on the decision taken by RRC. While the common channel is used, MAC-d passes data

to MAC-c/sh via the illustrated connection between MAC-d and MAC-c/sh. As a result, data received by MAC-d is delivered to the lower layer through either type of transport channels. We can also see that MAC-c/sh relieves data (which mostly consists of control information as paging one) from the higher layer directly and delivers them through the common transport channels.

Moreover, MAC measures the system state of RLC and MAC entities, and reports the measurement result to RRC. If the value representing the system state is out of the range set by RRC, RRC provides some control services for RLC or MAC. In this way, channel switching mentioned above and flow control can be performed. Details are found in [4].

3 Dynamic channel switching scheme

In this section, we introduce the dynamic channel switching scheme proposed for the architecture specified in the preceding section and [1]. This scheme provides control services (Channel switching and Flow control) based on the Buffer Occupancies (BOs) of transmission buffers in RLC and MAC entities.

Figure 5 shows the system architecture with data flows to downlinks. UTRAN is constructed from Node B (Base station) and RNC. As mentioned in the preceding section, RLC delivers RLC PDUs to MAC through a logical channel and MAC delivers these PDUs to Layer 1 through either type of transport channels. PDUs that belong to a particular data type (mainly control information) are always delivered through the common transport channel. And others are delivered in the following way.

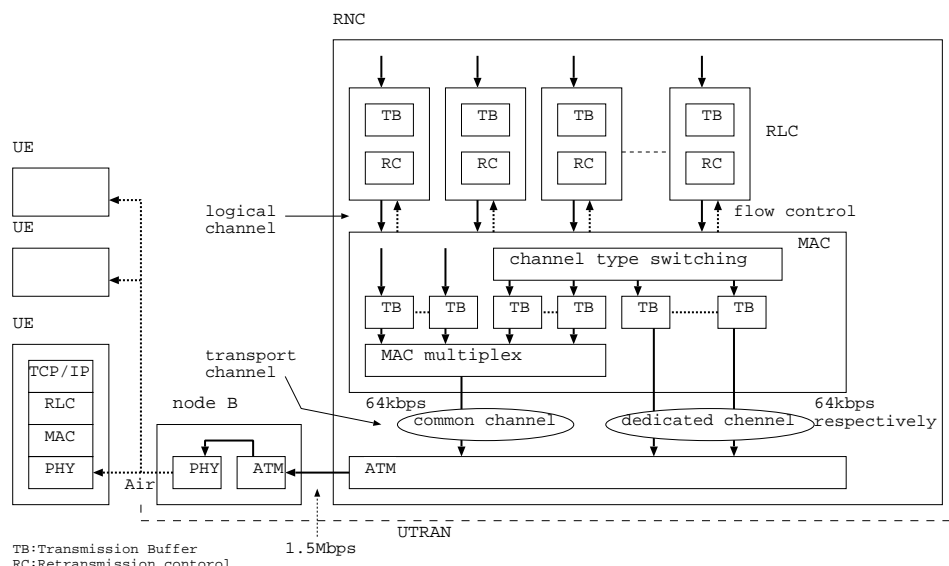


Figure 5: System architecture.

MAC receives these PDUs from RLC together with information which tells BOs of RLC transmission buffer. The value of BOs is reported to RRC, and RRC decides which type of

transport channels should be used for transmission based on the value. The common transport channel being used, the value higher than TH_u (Upper threshold set by RRC) causes channel switching to a dedicated transport channel only when it is available. On the other hand, a dedicated transport channel being used, the value lower than TH_l (Lower threshold set by RRC) causes channel switching to the common transport channel. As a rule, all of these PDUs are to be delivered through the common transport channel at first.

MAC also supports service multiplexing of higher layer PDUs into transport blocks delivered through common transport channel. They are served in a round-robin fashion, so that the PDUs waiting for transmission are accumulated in MAC transmission buffers. And then, the value of BOs of these buffers exceeding TH (Threshold set by RRC) causes the flow control. Under the control, the data flow from the connected RLC is limited.

We should notice that the value of BOs of RLC transmission buffers increases while the flow from RLC to MAC is being limited or retransmission service is being performed in RLC. In this thesis, we will disregard the retransmission service.

Now, we present the purpose of the dynamic channel switching scheme mentioned above. It enables us to use radio resources efficiently and economically and provides higher quality of data transmission as in the following way.

The common channel should be allocated to as many UEs as possible, since using a dedicated channel takes extra cost. A dedicated channel should be allocated to a UE that requests burst transmission beyond the capacity of the common channel. These channel allocations enable us to use radio resources efficiently and economically. Furthermore, the dynamic channel switching at an appropriate time prevents us from troubles caused by packet loss and provides higher quality of data transmission.

We should notice that the performance of these control services depends on the control parameters (TH_u, TH_l and TH). And appropriate values of the parameters that provide the most efficient use of radio resources and higher quality of data transmission have not been standardized yet. Thus, we present the performance analysis of the dynamic channel switching scheme in view of these parameters in this thesis.

4 Model description

In this section, we consider the mathematical model of the dynamic channel switching scheme described in the preceding section.

We first present a model that represents the dynamic channel switching system under some assumptions. Next we provide an approximate model that is to be analyzed in the sequel. In this thesis, a frame denotes the data unit treated in the system.

4.1 Dynamic channel switching model

4.1.1 Model introduction

Figure 6 represents the model structure of the dynamic channel switching system. Two stage queues, composed of RLC and MAC queues, are provided in the figure. We note that MAC

queues consist of dedicated MAC queues and a common MAC queue. The number of dedicated MAC queues is limited, since the number of dedicated channels is fixed.

Each of RLC queues has a buffer with capacity C_r frames. Each of dedicated MAC queues has a buffer with capacity C_m frames. The common MAC queue has as many buffers with capacity C_m frames as RLC queues.

Frames in each stream arrive at their own RLC queue. If a dedicated channel is allocated to a stream, frames in the stream are delivered to their own buffer of a dedicated MAC queue from RLC queue. If the common channel is allocated to a stream, frames in the stream are delivered to its own buffer of the common MAC queue from RLC queue.

Furthermore, dynamic channel allocations are performed as follows. All streams are allocated to the common channel at first. The channel type allocated to a stream is switched from the common channel to a dedicated channel if the RLC queue length is more than THu , given that an available dedicated channel exists. A channel switching from a dedicated channel to the common channel occurs if the RLC queue length is less than THl .

Flow controls are performed in the following way. If the queue length of the common MAC queue exceeds TH , the frames flow from the connected RLC queue is limited.

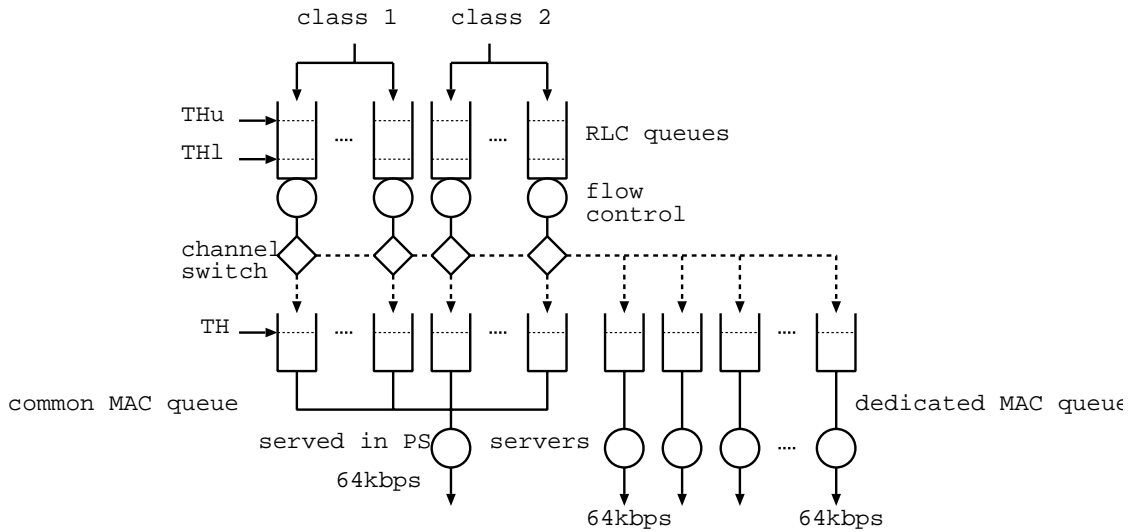


Figure 6: Dynamic channel switching model.

4.1.2 Assumptions on arrivals and services

We first provide some assumptions on the processes of arrival and service times in each queue.

A typical scenario for a fully utilized W-CDMA system includes a mixture of high-speed packet data users and low-rate voice connections. Thus, we consider two kinds of traffic to be arrived (see Figure 6). They are classified into two classes. We then assume that the stream of arrivals to class j ($j = 1, 2$) follows a Poisson process with rate λ_j .

Let the service time of a frame in a dedicated MAC buffer be exponentially distributed with rate μ . We assume that frames in common MAC buffers are served under the processor-sharing

service discipline. Then, the service time of a frame in a common MAC buffers is considered to be exponentially distributed with rate μ/N , where N denotes the number of active common MAC buffers. Furthermore, when the flow control is not performed, a frame in the RLC queue departs from the queue before the next frame arrives, since the service time is less than the interval of arrivals. Thus, the number of frames in a RLC queue increases only when the flow control is performed. We then assume that the flow from a RLC queue to the connected common MAC queue is stopped while the flow control being performed, and that a frame arrived at a RLC queue are delivered to the connected common MAC queue on its arrival.

It is anticipated that this model is too complicated to analyze. Thus, we provide an approximate model in the following subsection.

4.2 Approximate model

4.2.1 Model description

We previously stated that the number of frames in a RLC queue increases only when the flow control is performed. Thus, we simply regard the two-stage queues as single-stage queues whose capacity should be $K = Cr + TH$.

Now, we replace the model presented previously with the model shown in Figure 7. We note that queues connected between RLC and MAC are united in the approximate model. It differs from the original model as to the location where channel switching is performed, since the channels shown in Figure 7 are to be switched in the face of servers. But the whole performance of the model is expected to be close to the original one. Thus, we will provide the analysis of this model.

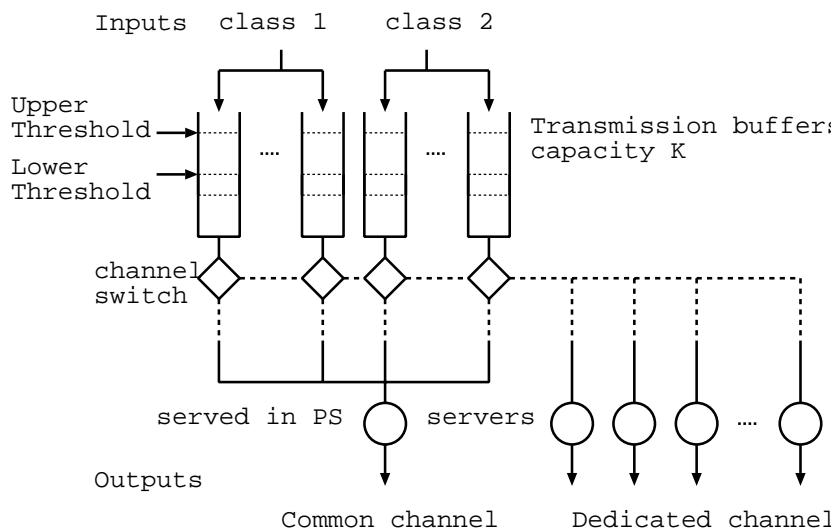


Figure 7: Approximate model.

We now consider two classes of arrival processes as shown in Section 4.1, and fix the number of class j streams to N_j ($j = 1, 2$). The number of buffers is $N_1 + N_2$. The capacity of each

buffer is $K (= Cr + TH)$. As to the thresholds, it is changed as follows: $T_U = THu + TH$ and $T_L = THl + TH$. The number of the dedicated channels is $D (\leq N_1 + N_2)$.

The behavior of the dynamic channel allocation is described as follows. All streams are allocated to the common channel at first. Frames in a stream arrive at their own buffer. The channel type allocated to a stream is switched from the common channel to a dedicated channel if the number of frames in the buffer is more than T_U , given that an available dedicated channel exists. Channel switching from a dedicated channel to the common channel occurs if the number of frames in the buffer is less than T_L . Furthermore, we provide the following assumption. In the case the number of buffers connected the common channel with their frames exceeding T_U is more than two, the probability that an available dedicated channel is allocated to a stream is equally likely.

4.2.2 Mathematical description

To analyze the model, we have to hold some random variables which represent the system state. Note, however, that holding all random variables which represent the model makes the analysis extremely complicated, even though we have already provided some approximations. Thus, we proceed as follows.

We now watch only one of these streams. The stream can be seen to be served at a queue with a varying service rate. We then provide the analysis focused on the tagged stream. As to other streams, we will hold a few random variables necessary to determine the service rate of the tagged queue. We then present some random variables that help describe the state of the tagged queue.

We first define k ($k = 0, 1, 2, \dots, K$) as the queue length of the tagged queue. We next define I as the class of streams the tagged stream belongs to. Thus, the arrival process of the stream is known as a Poisson process with rate λ_i , given that $I = i$.

To consider the process of service times, we define n_j ($j = 1, 2$) as the number of the class j streams allocated to dedicated channels except for the tagged one. We note that

$$n_1 + n_2 \leq D, \quad (1)$$

since the number of streams served at dedicated channels would not exceed D . We define $\gamma_j(i)$ as the maximum of n_j ($j = 1, 2$), given that $I = i$. Then, $\gamma_j(i)$ is given by

$$\gamma_j(i) = \begin{cases} \min\{D, N_j - 1\}, & \text{if } j = i, \\ \min\{D, N_j\}, & \text{if } j \neq i. \end{cases} \quad (2)$$

We note that $0 \leq n_j \leq \gamma_j(i)$.

Finally, we define t as

$$t = \begin{cases} 0, & \text{if the tagged stream is allocated the common channel,} \\ 1, & \text{if the tagged stream is allocated a dedicated channel.} \end{cases}$$

Let $r_j(n_j^*)$ ($j = 1, 2$) denote

$$r_j(n_j^*) = \Pr(k > 0 | I = j, n_j = n_j^*, t = 0), \quad (3)$$

and we assume that $r_j(n_j^*)$ ($j = 1, 2$) is given.

Then, the service time of a frame in the tagged queue is given as follows. It is distributed exponentially with rate $\mu(n_1, n_2, t)$. We define $\mu(n_1, n_2, t)$ as follows:

$$\mu(n_1, n_2, t) = \begin{cases} \mu/\{(N_1 - n_1)r_1(n_1) + (N_2 - n_2)r_2(n_2)\}, & \text{if } t = 0, \\ \mu, & \text{if } t = 1. \end{cases} \quad (4)$$

With the four random variables defined above and I , we can describe the state of the system approximately. In the following section, we present the analysis of this model.

5 Analysis

5.1 State set

We define $\omega = (k, n_1, n_2, t)$, which represents the state of the system. Let \mathcal{W}_i denote the whole state set of ω , given that $I = i$. The state set \mathcal{W}_i is defined by the following inequalities.

$$\begin{aligned} 0 \leq k \leq T_U - 1, & \quad 0 \leq n_1 \leq D - \gamma_2(i), \quad 0 \leq n_2 \leq \gamma_2(i), \quad t = 0, \\ 0 \leq k \leq T_U - 1, & \quad D - \gamma_2(i) + 1 \leq n_1 \leq \gamma_1(i), \quad 0 \leq n_2 \leq D - n_1, \quad t = 0, \\ T_U \leq k \leq K, & \quad D - \gamma_2(i) \leq n_1 \leq \gamma_1(i), \quad n_2 = D - n_1, \quad t = 0, \\ T_L + 1 \leq k \leq K, & \quad 0 \leq n_1 \leq D - \gamma_2(i) - 1, \quad 0 \leq n_2 \leq \gamma_2(i), \quad t = 1, \\ T_L + 1 \leq k \leq K, & \quad D - \gamma_2(i) \leq n_1 \leq \gamma_1(i), \quad 0 \leq n_2 \leq D - n_1 - 1, \quad t = 1. \end{aligned} \quad (5)$$

Figure 8 shows a subset of \mathcal{W}_i . The state space and transitions of (t, k) are represented in the figure. Note that the shaded states in the figure imply a failure of channel switching because of full-allocation of dedicated channels corresponding to shaded states in Figure 9.

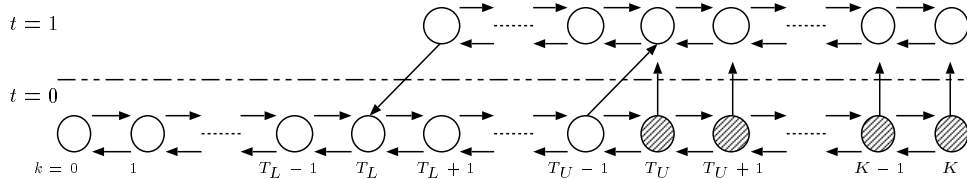


Figure 8: State set of t and k .

Figures 9 and 10 show subsets of \mathcal{W}_i . The state space and transitions of (n_1, n_2) are represented for $t = 0, 1$. Note that the sum of n_1 and n_2 is less than $D - 1$ in Figure 10, since a dedicated channel is allocated to the tagged stream. In the following section, we detail these state transitions.

5.2 State transitions

There are only a finite number of possible states. We assume that the sojourn time in each state is exponentially distributed. Thus ω forms a continuous-time finite-state Markov chain. In this section, we introduce some parameters necessary to describe the state transitions of the

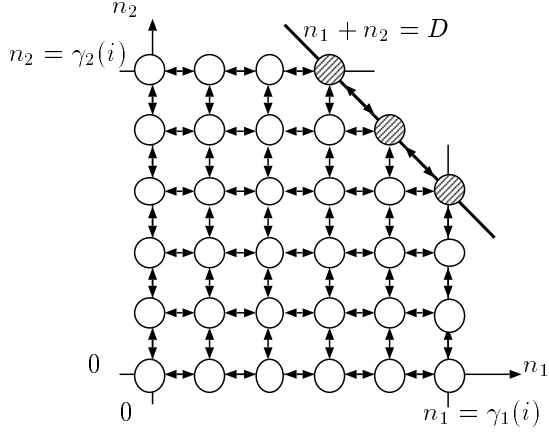


Figure 9: State set of n_1 and n_2 ($t=0$).

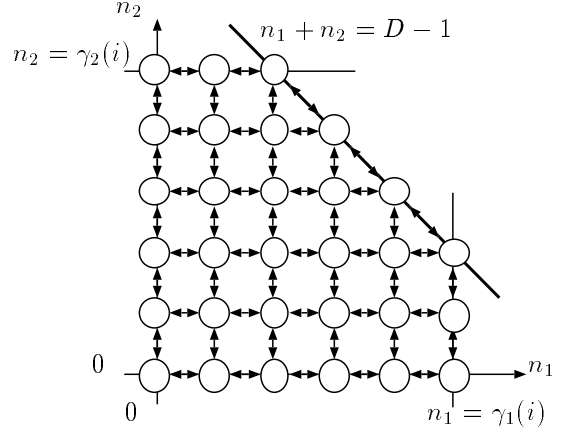


Figure 10: State set of n_1 and n_2 ($t=1$).

Markov chain. However, these parameters depends on the steady state probability. We assume that the steady state probability is given. We proceed as follows.

Let $\pi_{i,k^*,n_1^*,n_2^*,t^*}$ denote the steady state probability, which represents

$$\pi_{i,k^*,n_1^*,n_2^*,t^*} = \Pr(k = k^*, n_1 = n_1^*, n_2 = n_2^*, t = t^* | I = i). \quad (6)$$

Then, $r_j(n_j^*)$ provided in (3) is given by

$$r_j(n_j^*) = \frac{\sum_{\omega \in \mathcal{X}_{j,n_1^*}} \pi_{j,k,n_1,n_2,t}}{\sum_{\omega \in \mathcal{Y}_{j,n_1^*}} \pi_{j,k,n_1,n_2,t}},$$

where $\mathcal{X}_{j,n_1^*} = \{\omega ; k > 0, n_1 = n_1^*, t = 0, \omega \in \mathcal{W}_j\}$ and $\mathcal{Y}_{j,n_1^*} = \{\omega ; n_1 = n_1^*, t = 0, \omega \in \mathcal{W}_j\}$.

We then define θ_j ($j = 1, 2$) as

$$\theta_j = \frac{\sum_{\omega \in \mathcal{E}_{j,0}} \pi_{j,k,n_1,n_2,t}}{\sum_{\omega \in \mathcal{C}_j} \pi_{j,k,n_1,n_2,t}},$$

where $\mathcal{C}_j = \{\omega ; t = 0, \omega \in \mathcal{W}_j\}$ and $\mathcal{E}_{j,0} = \{\omega ; k \geq T_U, n_1 + n_2 = D, t = 0, \omega \in \mathcal{W}_j\}$. Note that θ_j ($j = 1, 2$) represents the probability that a class j stream is served in the common channel in spite of its queue length exceeding T_U because of full-allocation of dedicated channels.

We next define $c_j(i, n_1^*, t^*, l)$ as

$$c_j(i, n_1^*, t^*, l) = \frac{m_{i,j}!}{l!(m_{i,j} - l)!} \theta^l (1 - \theta_j)^{m_{i,j} - l},$$

where

$$m_{i,j} = \begin{cases} N_j - n_j^* - 1, & \text{if } j = i, \\ N_j - n_j^*, & \text{if } j \neq i, \end{cases} \quad (7)$$

$$n_2^* = \begin{cases} D - n_1^*, & \text{if } t^* = 0, \\ D - n_1^* - 1, & \text{if } t^* = 1. \end{cases} \quad (8)$$

Note that $c_j(i, n_1^*, t^*, l)$ represents the probability that the number of class j ($j = 1, 2$) streams served in the common channel with its queue length exceeding T_U is l , given that $I = i$, $n_1 = n_1^*$, $n_2 = n_2^*$ and $t = t^*$. Note that $m_{i,j}$ represents the number of class j streams served in the common channel, given that $I = i$. Note that the pair of n_1^* and n_2^* which satisfies (8) indicates the situation dedicated channels are fully allocated.

If dedicated channels are fully allocated, the streams served in the common channel with its queue length exceeding T_U must stay in the common channel till a dedicated channel becomes available. When a dedicated channel becomes available, the available channel is immediately allocated to a stream whose queue length exceeds T_U . We next introduce four types of probability necessary to describe such simultaneous transitions.

We first define $f_i(n_1^*, t^*)$ as

$$f_i(n_1^*, t^*) = c_1(i, n_1^*, t^*, 0)c_2(i, n_1^*, t^*, 0).$$

Note that $f_i(n_1^*, t^*)$ represents the probability that no channel switching occurs when a dedicated channel becomes available, given that $I = i$, $n_1 = n_1^*$ and $t = t^*$.

We define $d_i(n_1^*)$ as

$$d_i(n_1^*) = \sum_{l_1=0}^{m_{i,1}} \sum_{l_2=0}^{m_{i,2}} c_1(i, n_1^*, 0, l_1)c_2(i, n_1^*, 0, l_2) \frac{1}{l_1 + l_2 + 1},$$

where $m_{i,j}$ ($j = 1, 2$) satisfies (7). Note that $d_i(n_1^*)$ represents the probability that the tagged stream changes its channel type when a dedicated channel becomes available, given that $I = i$ and $n_1 = n_1^*$.

We define $g_{i,j}(n_1^*, t^*)$ as

$$g_{i,j}(n_1^*, t^*) = \sum_{l_1=\bar{l}_1(i)}^{m_{i,1}} \sum_{l_2=\bar{l}_2(i)}^{m_{i,2}} c_1(i, n_1^*, t^*, l_1)c_2(i, n_1^*, t^*, l_2) \frac{l_j}{l_1 + l_2},$$

where $\bar{l}_1(i)$ ($j = 1, 2$)

$$\bar{l}_j(i) = \begin{cases} 1, & \text{if } j = i, \\ 0, & \text{if } j \neq i. \end{cases}$$

and $m_{i,j}$ ($j = 1, 2$) satisfies (7). Note that $g_{i,j}(n_1^*, t^*)$ represents the probability that a class j stream changes its channel type when a dedicated channel becomes available, given that $I = i$, $n_1 = n_1^*$, $t = t^*$ and the tagged stream need not change its channel type.

We define $\hat{g}_{i,j}(n_1^*, t^*)$ as

$$\hat{g}_{i,j}(n_1^*, t^*) = \sum_{l_1=0}^{m_{i,1}} \sum_{l_2=0}^{m_{i,2}} c_1(i, n_1^*, t^*, l_1)c_2(i, n_1^*, t^*, l_2) \frac{l_j}{l_1 + l_2 + 1},$$

where $m_{i,j}$ ($j = 1, 2$) satisfies (7). Note that $\hat{g}_{i,j}(n_1^*, t^*)$ represents the probability that a class j stream changes its channel type when a dedicated channel becomes available, given that $I = i$, $n_1 = n_1^*$, $t = t^*$ and the tagged stream need change its channel type.

We next define $p_j(n_1^*, n_2^*, t^*)$ ($j = 1, 2$) as

$$p_1(n_1^*, n_2^*, t^*) = \begin{cases} \frac{\pi_{1,T_U-1,n_1^*,n_2^*,0}}{\sum_{k=0}^{T_U-1} \pi_{1,k,n_1^*,n_2^*,0}} \lambda_1, & \text{if } n_1^* + n_2^* < D \text{ and } t^* = 0, \\ \frac{\pi_{1,T_U-1,n_1^*+1,n_2^*,0}}{\sum_{k=0}^{T_U-1} \pi_{1,k,n_1^*+1,n_2^*,0}} \lambda_1, & \text{if } n_1^* + n_2^* < D - 1 \text{ and } t^* = 1, \end{cases}$$

$$p_2(n_1^*, n_2^*, t^*) = \begin{cases} \frac{\pi_{2,T_U-1,n_1^*,n_2^*,0}}{\sum_{k=0}^{T_U-1} \pi_{2,k,n_1^*,n_2^*,0}} \lambda_2, & \text{if } n_1^* + n_2^* < D \text{ and } t^* = 0, \\ \frac{\pi_{2,T_U-1,n_1^*,n_2^*+1,0}}{\sum_{k=0}^{T_U-1} \pi_{2,k,n_1^*,n_2^*+1,0}} \lambda_2, & \text{if } n_1^* + n_2^* < D - 1 \text{ and } t^* = 1. \end{cases}$$

Note that $p_j(n_1^*, n_2^*, t^*)$ represents the rate at which a channel switching to a dedicated channel occurs for a class j stream, given that $n_1 = n_1^*$, $n_2 = n_2^*$, $t = t^*$ and the number of available dedicated channels is more than one.

Let $1/q_j$ ($j = 1, 2$) represents the mean of service periods for class j streams in dedicated channels. As we know, a service period starts with a backlog of k ($T_U \leq k \leq K$) jobs. Thus the service period is equivalent to the sum of means of $k - T_U$ busy periods, the h th one having length b_{K-k+h} where b_n represents a mean length of a busy period in M/M/1/n queue. We define $B_{j,k}$ as a mean of the service period for class j stream with a backlog of k and it follows that

$$B_{j,k} = \sum_{n=K-k}^{K-T_U-1} b_{j,n}, \quad (9)$$

where $b_{j,n}$ is given in [6] as follows,

$$b_{j,n} = (b_{j,n-1} - \sum_{m=1}^{n-1} b_{j,m} c_{j,n-m}) / c_0, \quad n \geq 2, \quad (10)$$

$$c_{j,l} = \frac{1}{1 + \rho_j} \left(\frac{\rho_j}{1 + \rho_j} \right)^l, \quad l \geq 0,$$

and $b_{j,0} = 1/\mu$, $b_{j,1} = 1/\mu c_{j,0}$, $\rho_j = \lambda_j/\mu$.

We define a conditional probability $B_{j,k}^*$ ($T_U \leq k \leq K$) as

$$B_{j,k}^* = \Pr(\text{Service period starts with a backlog of } k \mid \text{Service period starts}). \quad (11)$$

To obtain $B_{j,k}^*$, we define $\bar{B}_{j,k}$ as the proportion of $B_{j,k}^*$ and it follows that

$$\bar{B}_{j,k} = \begin{cases} \sum_{\omega \in \mathcal{F}_{j,T_U}} \pi_{j,k,n_1,n_2,t} (n_1 q_1 + n_2 q_2) d_j(n_1) + \sum_{\omega \in \mathcal{G}_j} \pi_{j,k-1,n_1,n_2,t} \lambda_j, & \text{if } k = T_U, \\ \sum_{\omega \in \mathcal{F}_{j,k}} \pi_{j,k,n_1,n_2,t} (n_1 q_1 + n_2 q_2) d_j(n_1), & \text{if } T_U + 1 \leq k \leq K. \end{cases} \quad (12)$$

where $\mathcal{F}_{j,k^*} = \{\omega ; k = k^*, n_1 + n_2 = D, t = 0, \omega \in \mathcal{W}_j\}$ and $\mathcal{G}_j = \{\omega ; k = T_U - 1, n_1 + n_2 < D, t = 0, \omega \in \mathcal{W}_j\}$. Then, $B_{j,k}^*$ is obtained by

$$B_{j,k}^* = \frac{\bar{B}_{j,k}}{\sum_{l=T_U}^K \bar{B}_{j,l}}.$$

From $B_{j,k}$ and $B_{j,k}^*$, we obtain q_j by

$$q_j = \frac{1}{\sum_{k=T_U}^K B_{j,k}^* B_{j,k}}. \quad (13)$$

We note that q_1 and q_2 are necessary in (12) to obtain q_j ($j = 1, 2$) in (13). Therefore, we should compute q_j in the following procedure. Let a superscript of each parameter denote times of iterations.

Procedure to obtain q_j ($j = 1, 2$)

Step Q0: Choose $q_j^{[0]}$ ($j = 1, 2$) such that $q_j^{[0]} > 0$. Set $s = 0$.

Step Q1: Compute $B_{j,k}$ for $(j, k) \in \{j, k | j = 1, 2, k = T_U, T_U + 1, \dots, K\}$ by (9) and (10).

Step Q2: Set $s = s + 1$.

Step Q3: Obtain $\bar{B}_{j,k}^{[s]}$ for $(j, k) \in \{j, k | j = 1, 2, k = T_U, T_U + 1, \dots, K\}$ by

$$\bar{B}_{j,k}^{[s]} = \begin{cases} \sum_{\omega \in \mathcal{F}_{j,T_U}} \pi_{j,k,n_1,n_2,t} (n_1 q_1^{[s-1]} + n_2 q_2^{[s-1]}) d_j(n_1) + \sum_{\omega \in \mathcal{G}_j} \pi_{j,k-1,n_1,n_2,t} \lambda_j, & \text{if } k = T_U, \\ \sum_{\omega \in \mathcal{F}_{j,k}} \pi_{j,k,n_1,n_2,t} (n_1 q_1^{[s-1]} + n_2 q_2^{[s-1]}) d_j(n_1), & \text{if } T_U + 1 \leq k \leq K, \end{cases}$$

where $\mathcal{F}_{j,k^*} = \{\omega ; t = 0, k = k^*, n_1 + n_2 = D, \omega \in \mathcal{W}_j\}$ and $\mathcal{G}_j = \{\omega ; t = 0, k = T_U - 1, n_1 + n_2 < D, \omega \in \mathcal{W}_j\}$.

Step Q4: Obtain $B_{j,k}^{*[s]}$ for $(j, k) \in \{j, k | j = 1, 2, k = T_U, T_U + 1, \dots, K\}$ by

$$B_{j,k}^{*[s]} = \frac{\bar{B}_{j,k}^{[s]}}{\sum_{l=T_U}^K \bar{B}_{j,l}^{[s]}}.$$

Step Q5: Obtain $q_j^{[s]}$ ($j = 1, 2$) by

$$q_j^{[s]} = \frac{1}{\sum_{k=T_U}^K B_{j,k}^{*[s]} B_{j,k}}.$$

Step Q6: Let ε be enough small. If $\sum_{j=1}^2 \|q_j^{[s]} - q_j^{[s-1]}\| < \varepsilon$, we have the approximation $q_j^{[s]}$ ($j = 1, 2$) to the solution q_j ($j = 1, 2$), and otherwise, go to Step Q2.

Table 1 summarizes the source state transition of the Markov chain, given that $I = i$ and the source state is in (k, n_1, n_2, t) .

Table 1: Source state transition, given that $I = i$ and the source state is in (k, n_1, n_2, t) .

Destination	Rate	Condition
$(k + 1, n_1, n_2, t)$	λ_i	$k < K, k \neq T_U - 1$
		$k = T_U - 1, t = 1$
		$k = T_U - 1, t = 0, n_1 + n_2 = D$
$(k + 1, n_1, n_2, t + 1)$		$k = T_U - 1, t = 0, n_1 + n_2 < D$
$(k - 1, n_1, n_2, t)$	$\mu(n_1, n_2, t)$	$k > 0, t = 0$
		$k > T_L + 1, t = 1$
$(k - 1, n_1, n_2, t - 1)$	$\mu(n_1, n_2, t) f_i(n_1, t)$	$k = T_L + 1, n_1 + n_2 < D - 1, t = 1$
		$k = T_L + 1, n_1 + n_2 = D - 1, t = 1$
$(k - 1, n_1 + 1, n_2, t - 1)$	$\mu(n_1, n_2, t) g_{i,1}(n_1, t)$	$k = T_L + 1, n_1 + n_2 = D - 1, n_1 < \gamma_1(i), t = 1$
$(k - 1, n_1, n_2 + 1, t - 1)$	$\mu(n_1, n_2, t) g_{i,2}(n_1, t)$	$k = T_L + 1, n_1 + n_2 = D - 1, n_2 < \gamma_2(i), t = 1$
$(k, n_1 + 1, n_2, t)$	$(N_1 - n_1) p_1(n_1, n_2, t)$	$n_1 < \gamma_1(i), n_1 + n_2 < D, t = 0$
		$n_1 < \gamma_1(i), n_1 + n_2 < D - 1, t = 1$
$(k, n_1 - 1, n_2, t)$	$n_1 q_1$	$n_1 > 0, n_1 + n_2 < D, t = 0$
		$n_1 > 0, n_1 + n_2 < D - 1, t = 1$
	$n_1 q_1 f_i(n_1, t)$	$n_1 > 0, n_1 + n_2 = D, t = 0, k < T_U$
		$n_1 > 0, n_1 + n_2 = D - 1, t = 1$
$(k, n_1 - 1, n_2, t + 1)$	$n_1 q_1 d_1(n_1)$	$n_1 > 0, n_1 + n_2 = D, t = 0, k \geq T_U$
$(k, n_1 - 1, n_2 + 1, t)$	$n_1 q_1 \hat{g}_{i,1}(n_1, t)$	$n_1 > 0, n_2 < \gamma_2(i), n_1 + n_2 = D, t = 0, k \geq T_U$
		$n_1 > 0, n_2 < \gamma_2(i), n_1 + n_2 = D, t = 0, k < T_U$
		$n_1 > 0, n_2 < \gamma_2(i), n_1 + n_2 = D - 1, t = 1$
$(k, n_1, n_2 + 1, t)$	$(N_2 - n_2) p_2(n_1, n_2, t)$	$n_2 < \gamma_2(i), n_1 + n_2 < D, t = 0$
		$n_2 < \gamma_2(i), n_1 + n_2 < D - 1, t = 1$
$(k, n_1, n_2 - 1, t)$	$n_2 q_2$	$n_2 > 0, n_1 + n_2 < D, t = 0$
		$n_2 > 0, n_1 + n_2 < D - 1, t = 1$
	$n_2 q_2 f_i(n_1, t)$	$n_2 > 0, n_1 + n_2 = D, t = 0, k < T_U$
		$n_2 > 0, n_1 + n_2 = D - 1, t = 1$
$(k, n_1, n_2 - 1, t + 1)$	$n_2 q_2 d_2(n_1)$	$n_2 > 0, n_1 + n_2 = D, t = 0, k \geq T_U$
$(k, n_1 + 1, n_2 - 1, t)$	$n_2 q_2 \hat{g}_{i,2}(n_1, t)$	$n_2 > 0, n_1 < \gamma_1(i), n_1 + n_2 = D, t = 0, k \geq T_U$
		$n_2 > 0, n_1 < \gamma_1(i), n_1 + n_2 = D, t = 0, k < T_U$
		$n_2 > 0, n_1 < \gamma_1(i), n_1 + n_2 = D - 1, t = 1$

Remark: Transitions not described above would not occur, and the rates of such transitions are set to be 0.

5.3 Stationary equations

In the previous section, we consider the state transitions and provide the parameters necessary to provide transition rates, given that the steady state probability is known. In this section, we first consider how to obtain the steady state probability, given that the state transition rates described in Table 1 are known.

Let $\boldsymbol{\pi}_i$ denote the steady state probability vector, given that $I = i$. As noted previously, (k, n_1, n_2, t) forms a continuous-time Markov chain with finite states. Thus, if we solve the stationary equations

$$\boldsymbol{\pi}_i \mathbf{Q}_i = \mathbf{0}, \quad \boldsymbol{\pi}_i \mathbf{e} = 1, \quad (14)$$

we can obtain $\boldsymbol{\pi}_i$, where \mathbf{Q}_i denotes the infinitesimal generator of the Markov chain, given that $I = i$, and \mathbf{e} denotes a column vector of ones with an appropriate dimension. Note that \mathbf{Q}_i is denoted by

$$\mathbf{Q}_i = \{a_{\omega, \omega'}(i)\},$$

where $\omega \in \mathcal{W}_i$, $\omega' \in \mathcal{W}_i$ and

$$a_{\omega, \omega'}(i) = \begin{cases} \{\text{Transition rate from } \omega \text{ to } \omega'\} & \text{if } \omega' \neq \omega. \\ - \sum_{\omega^* \in \mathcal{W}_i, \omega^* \neq \omega} a_{\omega, \omega^*}(i) & \text{if } \omega' = \omega. \end{cases} \quad (15)$$

and these transition rates are given in Table 1. Thus, it is sure that $\boldsymbol{\pi}_i$ can be obtained, given that the state transition rates in Table 1 are known.

We next focus on the stationary equations. Note, however, that the state space will be large in general and the matrix \mathbf{Q}_i is sparse. Thus, it seems that the computational cost of any brute force method to solve (14) would be prohibitively large even for problems of moderate size. We explore the hierarchical structure of \mathbf{Q}_i , which helps reduce the computational cost in solving (14).

We then set the structure of the steady state probability vector $\boldsymbol{\pi}_i$ as follows:

$$\boldsymbol{\pi}_i = (\boldsymbol{\pi}_{i,0}, \boldsymbol{\pi}_{i,0}, \dots, \boldsymbol{\pi}_{i,k}, \dots, \boldsymbol{\pi}_{i,K}),$$

where $\boldsymbol{\pi}_{i,k}$ ($k = 0, 1, \dots, K$) consists of vectors as follows:

$$\boldsymbol{\pi}_{i,k} = (\boldsymbol{\pi}_{i,k,0}, \boldsymbol{\pi}_{i,k,1}, \dots, \boldsymbol{\pi}_{i,k,n_1}, \dots, \boldsymbol{\pi}_{i,k,\gamma_1(i)}).$$

Further $\boldsymbol{\pi}_{i,k,n_1}$ ($n_1 = 0, 1, \dots, \gamma_1(i)$) takes the form:

$$\boldsymbol{\pi}_{i,k,n_1} = (\boldsymbol{\pi}_{i,k,n_1,0}, \boldsymbol{\pi}_{i,k,n_1,1}, \dots, \boldsymbol{\pi}_{i,k,n_1,n_2}, \dots, \boldsymbol{\pi}_{i,k,n_1,n_2^*(i)}),$$

where $n_2^*(i)$ is given by

$$n_2^*(i) = \begin{cases} \gamma_2(i), & \text{if } n_1 \leq D - \gamma_2(i), \\ D - n_1, & \text{if } n_1 \geq D - \gamma_2(i) + 1. \end{cases} \quad (16)$$

Moreover, $\boldsymbol{\pi}_{i,k,n_1,n_2}$ ($n_2 = 0, 1, \dots, n_2^*(i)$) consists of elements denoted by $\pi_{i,k,n_1,n_2,t}$ whose subscripts satisfy $(k, n_1, n_2, t) \in \mathcal{W}_i$.

The structure of $\boldsymbol{\pi}_i$ described above makes \mathbf{Q}_i have a special hierarchal structure, since each random variable varies at most by one with any transition. The structure of \mathbf{Q}_i ($i = 1, 2$) is presented as follows:

$$\mathbf{Q}_i = \begin{pmatrix} \mathbf{S}_{i,0} & \mathbf{U}_{i,1} & & & \\ \mathbf{D}_{i,0} & \mathbf{S}_{i,1} & \mathbf{U}_{i,2} & & \\ & \ddots & \ddots & \ddots & \\ & & \mathbf{D}_{i,K-2} & \mathbf{S}_{i,K-1} & \mathbf{U}_{i,K} \\ & & & \mathbf{D}_{i,K-1} & \mathbf{S}_{i,K} \end{pmatrix},$$

where each block is constructed by the first level variable k . Note here that off-diagonal block matrices $\mathbf{D}_{i,k}$ ($k = 0, 1, \dots, K-1$) and $\mathbf{U}_{i,k}$ ($k = 1, 2, \dots, K$) take the following forms:

$$\mathbf{D}_{i,k} = \begin{pmatrix} \mathbf{S}_{i,k,0}^{(D)} & \mathbf{U}_{i,k,1}^{(D)} & & & \\ & \mathbf{S}_{i,k,1}^{(D)} & \mathbf{U}_{i,k,2}^{(D)} & & \\ & & \ddots & \ddots & \\ & & & \mathbf{S}_{i,k,\gamma_1(i)-1}^{(D)} & \mathbf{U}_{i,k,\gamma_1(i)}^{(D)} \\ & & & & \mathbf{S}_{i,k,\gamma_1(i)}^{(D)} \end{pmatrix},$$

$$\mathbf{U}_{i,k} = \begin{pmatrix} \mathbf{S}_{i,k,0}^{(U)} & & & & \\ & \mathbf{S}_{i,k,1}^{(U)} & & & \\ & & \ddots & & \\ & & & \mathbf{S}_{i,k,\gamma_1(i)-1}^{(U)} & \\ & & & & \mathbf{S}_{i,k,\gamma_1(i)}^{(U)} \end{pmatrix},$$

respectively. Furthermore, each diagonal block element $\mathbf{S}_{i,k}$ ($k = 0, 1, \dots, K$) takes the following form:

$$\mathbf{S}_{i,k} = \begin{pmatrix} \mathbf{S}_{i,k,0}^{(S)} & \mathbf{U}_{i,k,1}^{(S)} & & & \\ \mathbf{D}_{i,k,0}^{(S)} & \mathbf{S}_{i,k,1}^{(S)} & \mathbf{U}_{i,k,2}^{(S)} & & \\ & \ddots & \ddots & \ddots & \\ & & \mathbf{D}_{i,k,\gamma_1(i)-2}^{(S)} & \mathbf{S}_{i,k,\gamma_1(i)-1}^{(S)} & \mathbf{U}_{i,k,\gamma_1(i)}^{(S)} \\ & & & \mathbf{D}_{i,k,\gamma_1(i)-1}^{(S)} & \mathbf{S}_{i,k,\gamma_1(i)}^{(S)} \end{pmatrix}.$$

In general, the block matrices $\mathbf{S}_{i,k,n_1}^{(D)}$ ($n_1 = 0, 1, \dots, \gamma_1(i)$), $\mathbf{U}_{i,k,n_1}^{(D)}$ ($n_1 = 1, 2, \dots, \gamma_1(i)$) and $\mathbf{S}_{i,k,n_1}^{(U)}$ ($n_1 = 0, 1, \dots, \gamma_1(i)$) takes the following form:

$$\mathbf{S}_{i,k,n_1}^{(D)} = \begin{pmatrix} \mathbf{S}_{i,k,n_1,0}^{(D,S)} & \mathbf{U}_{i,k,1}^{(D,S)} & & & \\ & \mathbf{S}_{i,k,n_1,1}^{(D,S)} & \mathbf{U}_{i,k,n_1,2}^{(D,S)} & & \\ & & \ddots & \ddots & \\ & & & \mathbf{S}_{i,k,n_1,n_2^*(i)-1}^{(D,S)} & \mathbf{U}_{i,k,n_1,n_2^*(i)}^{(D,S)} \\ & & & & \mathbf{S}_{i,k,n_1,n_2^*(i)}^{(D,S)} \end{pmatrix},$$

$$\mathbf{U}_{i,k,n_1}^{(D)} = \begin{pmatrix} \mathbf{S}_{i,k,n_1,0}^{(D,U)} & & & & & \\ & \mathbf{S}_{i,k,n_1,1}^{(D,U)} & & & & \\ & & \ddots & & & \\ & & & \mathbf{S}_{i,k,n_1,n_2^*(i)-1}^{(D,U)} & & \\ & & & & \mathbf{S}_{i,k,n_1,n_2^*(i)}^{(D,U)} & \end{pmatrix},$$

$$\mathbf{S}_{i,k,n_1}^{(U)} = \begin{pmatrix} \mathbf{S}_{i,k,n_1,0}^{(U,S)} & & & & & \\ & \mathbf{S}_{i,k,n_1,1}^{(U,S)} & & & & \\ & & \ddots & & & \\ & & & \mathbf{S}_{i,k,n_1,n_2^*(i)-1}^{(U,S)} & & \\ & & & & \mathbf{S}_{i,k,n_1,n_2^*(i)}^{(U,S)} & \end{pmatrix},$$

where $n_2^*(i)$ is given in (16). Furthermore, matrices $\mathbf{S}_{i,k,n_1}^{(S)}$ ($n_1 = 0, 1, \dots, \gamma_1(i)$), $\mathbf{U}_{i,k,n_1}^{(S)}$ ($n_1 = 1, 2, \dots, \gamma_1(i)$) and $\mathbf{D}_{i,k,n_1}^{(S)}$ ($n_1 = 0, 1, \dots, \gamma_1(i) - 1$) take the form:

$$\mathbf{S}_{i,k,n_1}^{(S)} = \begin{pmatrix} \mathbf{S}_{i,k,n_1,0}^{(S,S)} & \mathbf{U}_{i,k,n_1,1}^{(S,S)} & & & & \\ \mathbf{D}_{i,k,n_1,0}^{(S,S)} & \mathbf{S}_{i,k,n_1,1}^{(S,S)} & \mathbf{U}_{i,k,n_1,2}^{(S,S)} & & & \\ & \ddots & \ddots & \ddots & & \\ & & \mathbf{D}_{i,k,n_1,n_2^*(i)-2}^{(S,S)} & \mathbf{S}_{i,k,n_1,n_2^*(i)-1}^{(S,S)} & \mathbf{U}_{i,k,n_1,n_2^*(i)}^{(S,S)} & \\ & & & \mathbf{D}_{i,k,n_1,n_2^*(i)-1}^{(S,S)} & \mathbf{S}_{i,k,n_1,n_2^*(i)}^{(S,S)} & \end{pmatrix},$$

$$\mathbf{U}_{i,k,n_1}^{(S)} = \begin{pmatrix} \mathbf{S}_{i,k,n_1,0}^{(S,U)} & & & & & \\ \mathbf{D}_{i,k,n_1,0}^{(S,U)} & \mathbf{S}_{i,k,n_1,1}^{(S,U)} & & & & \\ & \ddots & & & & \\ & & \mathbf{D}_{i,k,n_1,n_2^*(i)-2}^{(S,U)} & \mathbf{S}_{i,k,n_1,n_2^*(i)-1}^{(S,U)} & & \\ & & & \mathbf{D}_{i,k,n_1,n_2^*(i)-1}^{(S,U)} & \mathbf{S}_{i,k,n_1,n_2^*(i)}^{(S,U)} & \end{pmatrix},$$

$$\mathbf{D}_{i,k,n_1}^{(S)} = \begin{pmatrix} \mathbf{S}_{i,k,n_1,0}^{(S,D)} & \mathbf{U}_{i,k,n_1,1}^{(S,D)} & & & & \\ & \mathbf{S}_{i,k,n_1,1}^{(S,D)} & \mathbf{U}_{i,k,n_1,2}^{(S,D)} & & & \\ & & \ddots & & & \\ & & & \mathbf{S}_{i,k,n_1,n_2^*(i)-1}^{(S,D)} & \mathbf{U}_{i,k,n_1,n_2^*(i)}^{(S,D)} & \\ & & & & \mathbf{S}_{i,k,n_1,n_2^*(i)}^{(S,D)} & \end{pmatrix},$$

where $n_2^*(i)$ is given in (16).

Note that, in our notations, matrices $\mathbf{D}_{i,k}$ and $\mathbf{U}_{i,k}$ represent the transitions in which the first level variable k change its state to k from $k+1$ and $k-1$, respectively. On the other hand, $\mathbf{S}_{i,k}$ represents no transition as to k . Table 2 summarizes the transitions represented by these matrices.

Table 2: Transition matrices.

Matrix	Transition	Matrix	Transition
$\mathbf{U}_{i,k}$	$\{k-1\} \rightarrow \{k\}$	$\mathbf{U}_{i,k,n_1,n_2}^{(D,S)}$	$\{k+1, n_1, n_2-1\} \rightarrow \{k, n_1, n_2\}$
$\mathbf{D}_{i,k}$	$\{k+1\} \rightarrow \{k\}$	$\mathbf{S}_{i,k,n_1,n_2}^{(D,S)}$	$\{k+1, n_1, n_2\} \rightarrow \{k, n_1, n_2\}$
$\mathbf{S}_{i,k}$	$\{k\} \rightarrow \{k\}$	$\mathbf{S}_{i,k,n_1,n_2}^{(D,U)}$	$\{k+1, n_1-1, n_2\} \rightarrow \{k, n_1, n_2\}$
$\mathbf{S}_{i,k,n_1}^{(D)}$	$\{k+1, n_1\} \rightarrow \{k, n_1\}$	$\mathbf{S}_{i,k,n_1,n_2}^{(U,S)}$	$\{k-1, n_1, n_2\} \rightarrow \{k, n_1, n_2\}$
$\mathbf{U}_{i,k,n_1}^{(D)}$	$\{k+1, n_1-1\} \rightarrow \{k, n_1\}$	$\mathbf{D}_{i,k,n_1,n_2}^{(S,S)}$	$\{k, n_1, n_2+1\} \rightarrow \{k, n_1, n_2\}$
$\mathbf{S}_{i,k,n_1}^{(U)}$	$\{k-1, n_1\} \rightarrow \{k, n_1\}$	$\mathbf{U}_{i,k,n_1,n_2}^{(S,S)}$	$\{k, n_1, n_2-1\} \rightarrow \{k, n_1, n_2\}$
$\mathbf{S}_{i,k,n_1}^{(S)}$	$\{k, n_1\} \rightarrow \{k, n_1\}$	$\mathbf{S}_{i,k,n_1,n_2}^{(S,S)}$	$\{k, n_1, n_2\} \rightarrow \{k, n_1, n_2\}$
$\mathbf{U}_{i,k,n_1}^{(S)}$	$\{k, n_1-1\} \rightarrow \{k, n_1\}$	$\mathbf{S}_{i,k,n_1,n_2}^{(S,U)}$	$\{k, n_1-1, n_2\} \rightarrow \{k, n_1, n_2\}$
$\mathbf{D}_{i,k,n_1}^{(S)}$	$\{k, n_1+1\} \rightarrow \{k, n_1\}$	$\mathbf{D}_{i,k,n_1,n_2}^{(S,U)}$	$\{k, n_1-1, n_2+1\} \rightarrow \{k, n_1, n_2\}$
		$\mathbf{U}_{i,k,n_1,n_2}^{(S,D)}$	$\{k, n_1+1, n_2-1\} \rightarrow \{k, n_1, n_2\}$
		$\mathbf{S}_{i,k,n_1,n_2}^{(S,D)}$	$\{k, n_1+1, n_2\} \rightarrow \{k, n_1, n_2\}$

6 Numerical algorithm

In general, we can obtain the steady state probability by solving stationary equations. However, in this thesis, the stationary equations are given in terms of the steady state probability. Thus, we provide an iterative algorithm to obtain the steady state probability as follows. Let superscripts of vectors and matrices denote times of iterations.

Iteration Procedure

Step I0: Let $\pi_i^{[0]}$ ($i = 1, 2$) be an uniform distribution.

Step I1: Set $n = 0$ and $i = 0$.

Step I2: Set $n = n + 1$.

Step I3: Change i as follows:

$$i = \begin{cases} 1, & \text{if } i \neq 1, \\ 2, & \text{if } i = 1. \end{cases}$$

Step I4: If $i = 1$, compute the parameters necessary to describe the Markov chain introduced in section 5.2 with $\pi_1^{[n]}$ and $\pi_2^{[n]}$, and otherwise, compute them with $\pi_1^{[n]}$ and $\pi_2^{[n-1]}$. Construct $\mathbf{Q}_i^{[n]}$ whose components follow the transition rates described in Table 1.

Step I5: Solve $\pi_i^{[n]} \mathbf{Q}_i^{[n]} = \mathbf{0}$ ($i = 1, 2$) and normalize $\pi_i^{[n]}$ to be $\pi_i^{[n]} \mathbf{e} = 1$.

Step I6: If $i = 1$, go to Step I3.

Step I7: Let ε be enough small. If $\sum_{i=1}^2 \|\pi_i^{[n]} - \pi_i^{[n-1]}\| < \varepsilon$, we have the approximation $\pi_i^{[n]}$ ($i = 1, 2$) to the solution π_i ($i = 1, 2$), and otherwise, go to Step I2.

In Step I5, we have to solve the stationary equations. It seems quite bother to solve large numbers of simultaneous equations. We next present the efficient procedure called RPA which takes account of the special hierarchical structure of $\mathbf{Q}_i^{[n]}$. Let a superscript $[n, m]$ indicate the m th iteration in RPA to solve $\pi_i^{[n]} \mathbf{Q}_i^{[n]} = \mathbf{0}$ ($i = 1, 2$) in Step I5.

Replacement Process Approach

Step R0: Let $\pi_i^{[n,0]} = \pi_i^{[n-1]}$ and $m = 0$.

Step R1: Set $m = m + 1$.

Step R2: For $(k, n_1, n_2) \in \{k, n_1, n_2 ; (k, n_1, n_2, t) \in \mathcal{W}_i\}$, solve $\pi_{i,k,n_1,n_2}^{*[n,m]} \mathbf{A}_{i,k,n_1,n_2}^{[n,m]} = \mathbf{0}$ and normalize $\pi_{i,k,n_1,n_2}^{*[n,m]}$ to be $\pi_{i,k,n_1,n_2}^{*[n,m]} \mathbf{e} = 1$, where $\pi_{i,k,n_1,n_2}^{*[n,m]}$ is defined as follows:

$$\begin{aligned} \pi_{i,k,n_1,n_2}^{*[n,m]} &= \frac{\pi_{i,k,n_1,n_2}^{[n,m]}}{\bar{\pi}_{i,k,n_1,n_2}^{[n,m]}}, \\ \bar{\pi}_{i,k,n_1,n_2}^{[n,m]} &= \pi_{i,k,n_1,n_2}^{[n,m]} \mathbf{e}, \end{aligned}$$

and $\mathbf{A}_{i,k,n_1,n_2}^{[n,m]}$ takes the form:

$$\mathbf{A}_{i,k,n_1,n_2}^{[n,m]} = \mathbf{S}_{i,k,n_1,n_2}^{[n](S,S)} + \mathbf{t}_{i,k,n_1,n_2}^{[n]} \frac{\mathbf{f}_{i,k,n_1,n_2}^{[n,m]}}{\mathbf{f}_{i,k,n_1,n_2}^{[n,m]}} \mathbf{e},$$

where vectors $\mathbf{t}_{i,k,n_1,n_2}^{[n]}$ and $\mathbf{f}_{i,k,n_1,n_2}^{[n,m]}$ is given as follows:

$$\begin{aligned} \mathbf{t}_{i,k,n_1,n_2}^{[n]} &= \mathbf{U}_{i,k-1,n_1,n_2+1}^{[n](D,S)} \mathbf{e} + \mathbf{U}_{i,k,n_1,n_2+1}^{[n](S,S)} \mathbf{e} + \mathbf{U}_{i,k,n_1-1,n_2+1}^{[n](S,D)} \mathbf{e} + \mathbf{D}_{i,k,n_1,n_2-1}^{[n](S,S)} \mathbf{e} \\ &\quad + \mathbf{D}_{i,k,n_1+1,n_2-1}^{[n](S,U)} \mathbf{e} + \mathbf{S}_{i,k-1,n_1,n_2}^{[n](D,S)} \mathbf{e} + \mathbf{S}_{i,k-1,n_1+1,n_2}^{[n](D,U)} \mathbf{e} + \mathbf{S}_{i,k+1,n_1,n_2}^{[n](U,S)} \mathbf{e} \\ &\quad + \mathbf{S}_{i,k,n_1+1,n_2}^{[n](S,U)} \mathbf{e} + \mathbf{S}_{i,k,n_1-1,n_2}^{[n](S,D)} \mathbf{e}, \end{aligned} \quad (17)$$

$$\begin{aligned} \mathbf{f}_{i,k,n_1,n_2}^{[n,m]} &= \pi_{i,k+1,n_1,n_2-1}^{[n,m-1]} \mathbf{U}_{i,k,n_1,n_2}^{[n](D,S)} + \pi_{i,k,n_1,n_2-1}^{[n,m-1]} \mathbf{U}_{i,k,n_1,n_2}^{[n](S,S)} \\ &\quad + \pi_{i,k,n_1+1,n_2-1}^{[n,m-1]} \mathbf{U}_{i,k,n_1,n_2}^{[n](S,D)} + \pi_{i,k,n_1,n_2+1}^{[n,m-1]} \mathbf{D}_{i,k,n_1,n_2}^{[n](S,S)} \\ &\quad + \pi_{i,k,n_1-1,n_2+1}^{[n,m-1]} \mathbf{D}_{i,k,n_1,n_2}^{[n](S,U)} + \pi_{i,k+1,n_1,n_2}^{[n,m-1]} \mathbf{S}_{i,k,n_1,n_2}^{[n](D,S)} \\ &\quad + \pi_{i,k+1,n_1-1,n_2}^{[n,m-1]} \mathbf{S}_{i,k,n_1,n_2}^{[n](D,U)} + \pi_{i,k-1,n_1,n_2}^{[n,m-1]} \mathbf{S}_{i,k,n_1,n_2}^{[n](U,S)} \\ &\quad + \pi_{i,k,n_1-1,n_2}^{[n,m-1]} \mathbf{S}_{i,k,n_1,n_2}^{[n](S,U)} + \pi_{i,k,n_1+1,n_2}^{[n,m-1]} \mathbf{S}_{i,k,n_1,n_2}^{[n](S,D)}. \end{aligned} \quad (18)$$

Remark: Note that vectors $\mathbf{t}_{i,k,n_1,n_2}^{[n]}$ and $\mathbf{f}_{i,k,n_1,n_2}^{[n,m]}$ may not consist of all the factors on the right hand side of (17) and (18). For example, $\mathbf{U}_{i,k-1,n_1,n_2+1}^{[n](D,S)}$, $\mathbf{S}_{i,k-1,n_1,n_2}^{[n](D,S)}$, $\mathbf{S}_{i,k-1,n_1+1,n_2}^{[n](D,U)}$ and $\pi_{i,k-1,n_1,n_2}^{[n,m-1]}$ do not exist for $k = 0$, so that we have to remove the factors including $\mathbf{U}_{i,k-1,n_1,n_2+1}^{[n](D,S)}$, $\mathbf{S}_{i,k-1,n_1,n_2}^{[n](D,S)}$, $\mathbf{S}_{i,k-1,n_1+1,n_2}^{[n](D,U)}$ and $\pi_{i,k-1,n_1,n_2}^{[n,m-1]}$ from the right hand side of (17) and (18) in the case $k = 0$.

7 Numerical results

Table 3 summarizes parameters used in numerical experiments. The load $\rho = (\lambda_1 N_1 + \lambda_2 N_2)/(\mu D + \mu)$ of the whole system was set to 15/16. Furthermore, the number D of dedicated channels is equal to the number N_1 of class 1 streams. Therefore, the performance of the system will be effectively improved by an appropriate channel allocation.

Table 3: Simulation Parameters.

Parameter	Value	Description
N_1	5 streams	Number of class 1 streams
N_2	10 streams	Number of class 2 streams
λ_1	60	Arrival rate of class 1 streams
λ_2	6	Arrival rate of class 2 streams
μ	64	Service rate of MAC servers
D	5 channels	Number of dedicated channels
C_m	48 frames	Capacity of MAC transmission buffers
TH	2 frames	Threshold for flow control
THu	<i>variable</i>	Upper threshold for channel switching
THl	2 frames	Lower threshold for channel switching

7.1 Efficiency of the proposed numerical procedure

We first discuss the efficiency achieved by applying the iterative algorithm RPA in solving the stationary equations. To appreciate the efficiency of RPA, two types of methods are applied to solve the stationary equations, i.e., RPA and LU decomposition given in [8].

Table 1 shows the time taken in solving the stationary equations with these two methods, given that $THu = 23$. Remember that we have to solve the stationary equations iteratively until the obtained steady state probability satisfies $\sum_{i=1}^2 \|\pi_i^{[n]} - \pi_i^{(n-1)}\| < \varepsilon$, as specified in section 6. In this specific case, we solved the stationary equations 32 times.

We can make sure that it is considerably efficient to apply RPA compared with the case LU decomposition is applied. Furthermore, in the case RPA is applied, the time taken in solving the stationary equations becomes smaller as the number of iterations increases. It implies that the value of $\sum_{i=1}^2 \|\pi_i^{[n]} - \pi_i^{(n-1)}\|$ becomes small as n increases.

Table 4: Time taken in solving stationary equations.

Times of iteration	RPA	LU decomposition
1	39 sec	94 sec
2	16	95
3	13	94
4	13	94
\vdots	\vdots	\vdots
31	7	93
32	6	94
Total	328	3060

7.2 Accuracy of approximate model

In this section, we describe the accuracy of the approximate model proposed in this thesis. In Figures 11, 12 and 13, the performance measures are represented with the results obtained simulation experiments of the original model. From these figures, we observe that the approximate model clearly suit the original one. Therefore, we can estimate the performance of the channel switching system, analyzing the approximate model we proposed in this thesis.

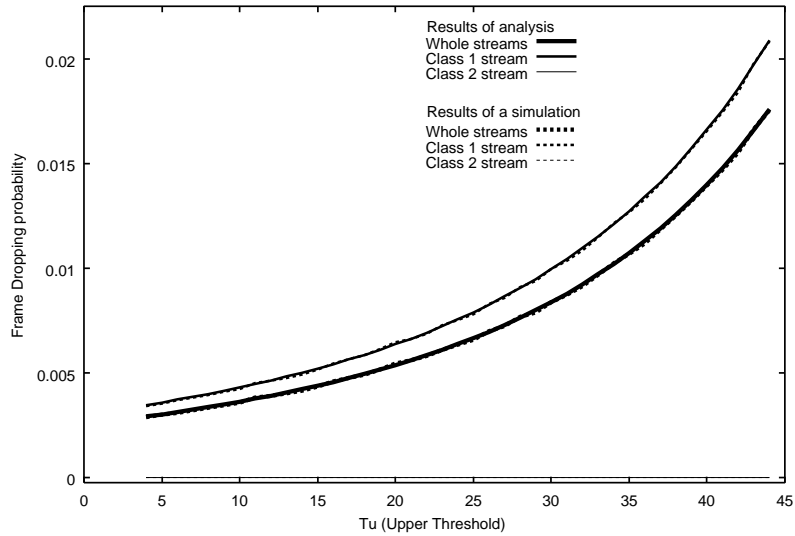


Figure 11: Frame dropping probability.

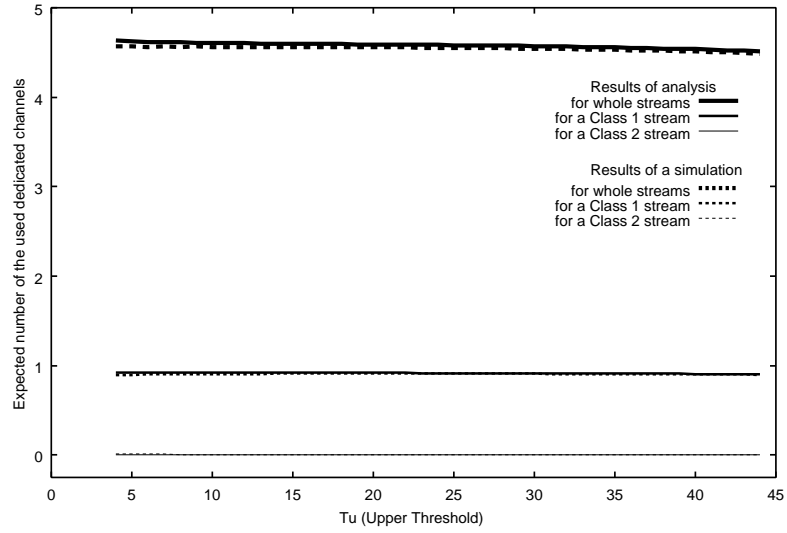


Figure 12: Expected number of used dedicated channels.

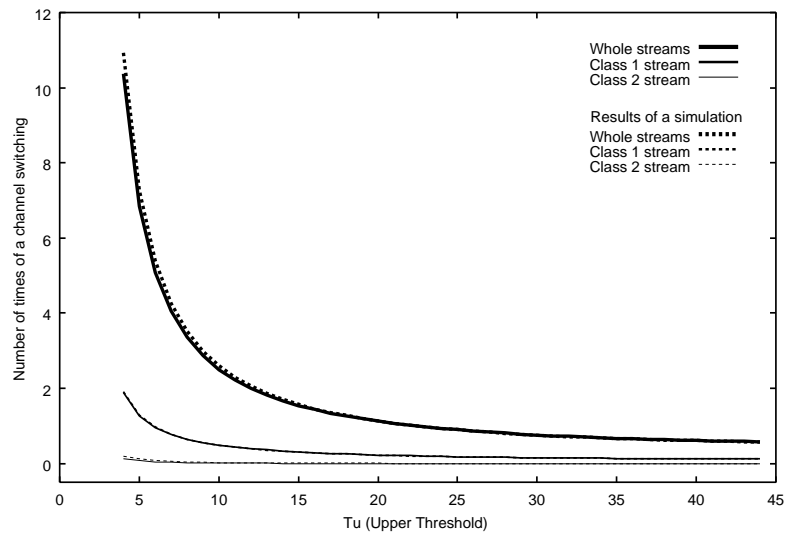


Figure 13: Frequency of channel switching per unit time.

7.3 Impact of upper threshold

As mentioned previously, the performance of the system may be effectively improved based on the channel allocation. Furthermore, the channel allocation is certainly dependent on the value of the upper threshold for channel switching. In this section, we will examine quantitative performance of the system, i.e., the frame dropping probability, the load of dedicated channels and the frequency of channel switchings.

We first focus on the frame dropping probability which is an important measure to estimate the quality of service provided to end users. In Figure 14, the frame dropping probability against the upper threshold THu are plotted. From this figure, we observe that a smaller THu is preferable for the purpose of minimizing the frame dropping probability. It implies that the large THu may cause the queue length to be long, so that the frame dropping probability becomes large.

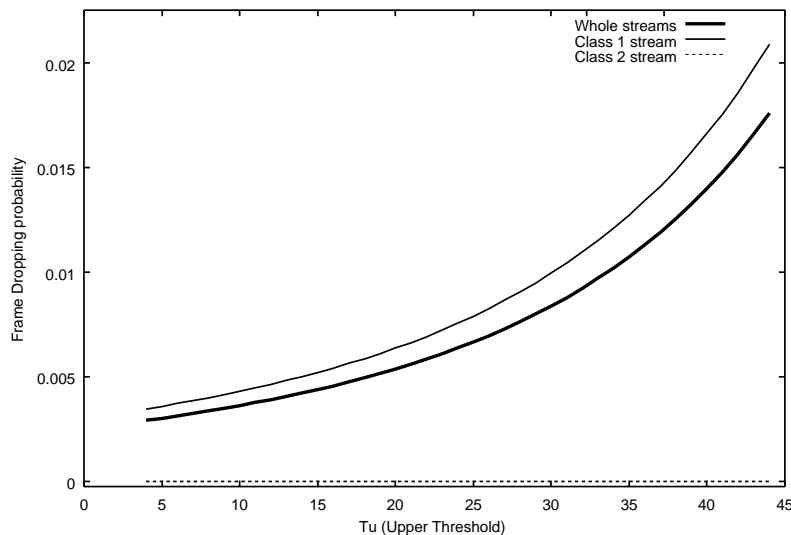


Figure 14: Frame dropping probability.

We next consider the load of dedicated channels. In Figure 15, the expected number of used dedicated channels is plotted. From this figure, we can observe that a larger THu is a little preferable for the purpose of minimizing the allocation of dedicated channels. However, it seems that the effect of the choice of the upper threshold is small. It implies that the amount of dropped frames caused by the larger THu is not large enough to reduce the load of the whole system, so that the load of dedicated channels stay high even if the upper threshold are set to be large.

Finally, we consider the frequency of channel switching per unit time. The overhead caused by channel switching is desired to be as small as possible. Therefore, the upper threshold should be set to reduce the frequency of channel switching. From Figure 16, we observe that a larger THu is certainly preferable for the purpose of minimizing the frequency of channel switching.

Note that a larger upper threshold effectively reduces the frequency of channel switchings, even though it dose not reduce the load of dedicated channels well. It implies that the service period in a dedicated channel becomes long when the value of THu is set large.

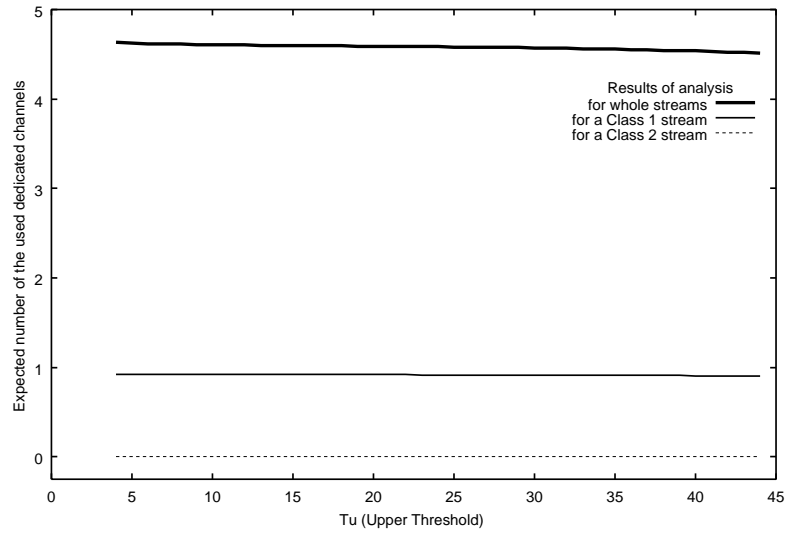


Figure 15: Expected number of used dedicated channels.

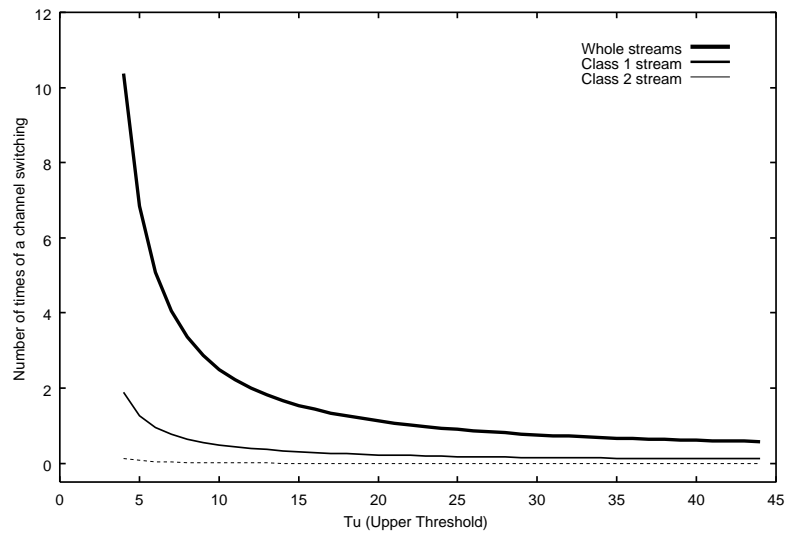


Figure 16: Frequency of channel switching per unit time.

8 Conclusion

In this thesis, we proposed an approximate model of the dynamic channel switching system. Furthermore, we described the model by a continuous-time finite-state Markov chain, and then we applied the efficient procedure called RPA to solve the stationary equations of the Markov chain.

Through numerical experiments, we examined quantitative performance of the system, i.e., the frame dropping probability, the load of a dedicated channel and the frequency of channel switching. Those results showed that the choice of the values of the thresholds has a great effect on the frame dropping probability and the frequency of channel switching, though it has a small effect on the load of a dedicated channel. Using those results, we can choose the appropriate values of the thresholds to realize the demanded performance of the system.

Acknowledgement

I would like to show a great deal of appreciation to Associate Professor Tetsuya Takine for his warm guidance and significant suggestions to accomplish this thesis. His words with plenty of wits and heart have greatly encouraged me. This thesis owes much to the thoughtful and helpful comments of him. I would like to express my gratitude to Professor Masao Fukushima for valuable suggestions and comments on several points of this thesis. Thanks are due to Mr. Yoshiaki Oota of Kyushu Institute of Technology for providing me helpful advice. He is also the one who evaluates the performance of the dynamic channel switching scheme in partnership with me. I also wish to thank students in Professor Fukushima's Laboratory for their support. Especially, I am deeply indebted to Mr. Hiroyuki Masuyama for his heartfelt encouragement, valuable advice and the pleasant time spent to relax. I am grateful to Yujin Imagawa for apt criticisms on several points in this thesis. Furthermore, I wish to thank Akihiro Enomoto for providing me comfortable surroundings to carry out computational experiments. Finally, special thanks are due to my parents and my sister for supporting me all the time.

I wish to start the life as a working member of society with all these thanks in my mind.

References

- [1] 3GPP, <http://www.3gpp.org/>.
- [2] 3GPP, "UMTS Access Stratum; Services and Function," 3G TS 23.110, ver.3.4.0, March 2000.
- [3] 3GPP, "Radio Interface Protocol Architecture," 3G TS 25.301, ver.3.7.0, March 2001.
- [4] 3GPP, "MAC protocol Specification," 3G TS 25.321, ver.3.7.0, March 2001.
- [5] 3GPP, "RLC protocol Specification," 3G TS 25.322, ver.3.6.0, December 2000.

- [6] L. W. Miller, “A Note on the Busy Period of an M/G/1 Finite Queue,” *Operations Research*, vol. 23, pp. 1179–1182, March 1975.
- [7] T. Takine, “Introduction to Numerical Solution Techniques of Finite-State Markov Chains and Its Applications,” Third Draft, December 1997.
- [8] W. H. Press, B. P. Flannery, S. A. Teukolsky and W. T. Vetterling, *Numerical RECIPES in C*, Cambridge University Press, New York, 1988.